

SLDCNet: Skin lesion detection and classification using full resolution convolutional network-based deep learning CNN with transfer learning

P. Bharat Siva Varma¹  | Siddartha Paturu² | Suman Mishra³ | B. Srinivasa Rao⁴ |
Pala Mahesh Kumar³  | Namani Vamshi Krishna⁵

¹Department of Computer Science and Engineering, Sagi Rama Krishnam Raju Engineering College, Bhimavaram, India

²Department of Data Science, World Bank Group, Washington, District of Columbia, USA

³Department of Electronics and Communication Engineering, CMR Engineering College, Hyderabad, India

⁴Department of Computer Science and Information Technology, Koneru Lakshmaiah Education Foundation, Guntur, India

⁵Department of Artificial Intelligence, SAK Informatics, Hyderabad, India

Correspondence

Pala Mahesh Kumar, Department of Electronics and Communication Engineering, CMR Engineering College, Kandlakoya, Hyderabad, India.

Email: maheshpala25@gmail.com;
palamahesh2103@aol.com

Abstract

Background: Skin cancer is one of the life threatening diseases in the world. So, millions of lives can be saved by early detection of skin cancer. In addition, automating the computer-aided system of skin lesion detection and classification (SLDC) will assist the medical practitioners to ensure more efficacious treatment of skin lesion disease.

Material and Method: In this article, a hybrid preprocessing-based transfer learning model for SLDC is proposed, which is named as SLDCNet. Initially, the hybrid Gaussian filter (HGF) with connected component label (CCL) based fast march inpainting procedure is used for hair removal and denoising of skin lesions. Next, full resolution convolutional networks (FrCN) based segmentation method is adapted for detecting the cancer region. Then, feature extraction is performed using deep residual learning and finally, transfer learning mechanism is applied for classification of eight skin lesions.

Results: The extensive simulation results shows that proposed SLDCNet resulted in a classification accuracy of 99.92%, sensitivity of 99%, and specificity of 99.36%, respectively.

Conclusion: From the obtained results, it is proven that proposed SLDCNet provides better performance as compared to state-of-art SLDC approaches, and even the standard ISIC-2019 public challenge.

KEY WORDS

fast march inpainting, fully resolution convolutional neural networks, gamma regularizer, hybrid Gaussian filter, skin lesion detection

1 | INTRODUCTION

Skin cancer has recently risen to the top of the list of malignancies that people are concerned about, and it is divided into benign and malignant categories (Thomsen et al., 2020). Benign tumours grow slowly and rarely spread. Malignant tumours can spread throughout the body, penetrate and destroy near the area normal tissues, and grow quickly. Melanoma is the deadliest class of these two types of skin cancers when compared to non-melanoma class. Melanoma can transmit to parts of your body from where it started. This is known as advanced Disease melanoma, or sophisticated. It has the chance to transmit to your respiratory tract, spleen, central nervous system, bone fragments, digestive tract, and lymph. The majority of the people explore their epidermis cancer at an early stage, once it has spread. Melanoma affects an increasing number of people year after year, and early treatment is critical for the endurance of patients. Usually, dermatologists with a lot of experience are required to

inspect the malignant melanoma. However, these individuals employed a computer-assisted approach to detect the melanoma at the earliest (Maiorino et al., 2016). Therefore, achieving higher accuracies have become a difficult undertaking due to the various challenges in SLDC. Many researchers have used image preprocessing to detect skin cancer at an early stage, allowing for more successful therapy. In order to increase the scope of such critical diagnostic treatment, effective frameworks for skin disease classification must be established. Various works are performed on skin cancer detection and classification operation. Doctor may examine your skin to determine whether the changes you are experiencing are the result of skin cancer. Extensive testing could be made to ensure that diagnostic test. Collect a piece of suspect surface for testing. Your doctor may start by removing the suspicious-looking skin for test results in the lab. Thus, International Skin Imaging Collaboration (ISIC) started the challenges (Gutman et al., 2016), (Murphree & Ngufor, 2017), (Codella et al., 2019) from the year 2016, so the performance of the participated teams (works) is officially verified. For improving the segmentation and classification accuracy, they also released standard datasets. By this challenge, various authors show their interest towards development of new architectures using DL and machine learning approaches. Various hospitals in worldwide implementing the methods obtained from leadership board of these challenges. Thus, it improves the survival rate of an individual patient. The initial process of skin cancer detection is pre-processing with respect to the noise removal and hair artefact removal (Talavera-Martínez et al., 2019). But these preprocessing and segmentation approaches performance is mainly suffering with various challenges of skin lesion. Figure 1 presents the various challenges (Goyal et al., 2020) presented in the real time scenarios. They are frame artefact, hair artefact, ruler mark artefact, bubbles, colour illumination, blood vessels, low contrast, and irregular fuzzy rules. Here, the white colour boundary represents the skin lesion segmented by the dermatologists.

Thus, the pre-processing plays the major role in removal these artefacts. Initially, edge detection (Jagadesh et al., 2020)-based methods were used to identify the artefacts. In addition, the impaired area can also be detected using the edge detection techniques such as prewitt, and sobel filters.

Then after, morphology-based approaches have been introduced, especially for hair removal from skin lesion images. It has couple of phases, where the foreground is removed in the first phase using the opening operation, while the background is removed in the latter phase using the closing operation. The obtained resultant from morphological operation (Abbas & Abu-Almash, 2020) (i.e., hair removed skin lesion image) can be aided in subsequent processing of skin lesion classification. Finally, the prewitt, and sobel edge detector filters are employed to find the edges. The Prewitt operator gives two masks, one for edge detection in the horizontal plane and one for detecting edges in the vertical plane. The Sobel filter is being used to detect the edges. It calculates the gradient of pixel intensities at each pixel of an image. It defines the direction of the largest increases in brightness from white to black and the rate of growth in that path. These morphological operation-based edge detection algorithms have poor objective and subjective classification. Usage of several filtering methods (Hemalatha et al., 2017) such as median average, Gaussian, bi-lateral, tri-lateral and wavelet filters can improve the efficiency of classification system by estimating the value of nearby pixel in order to

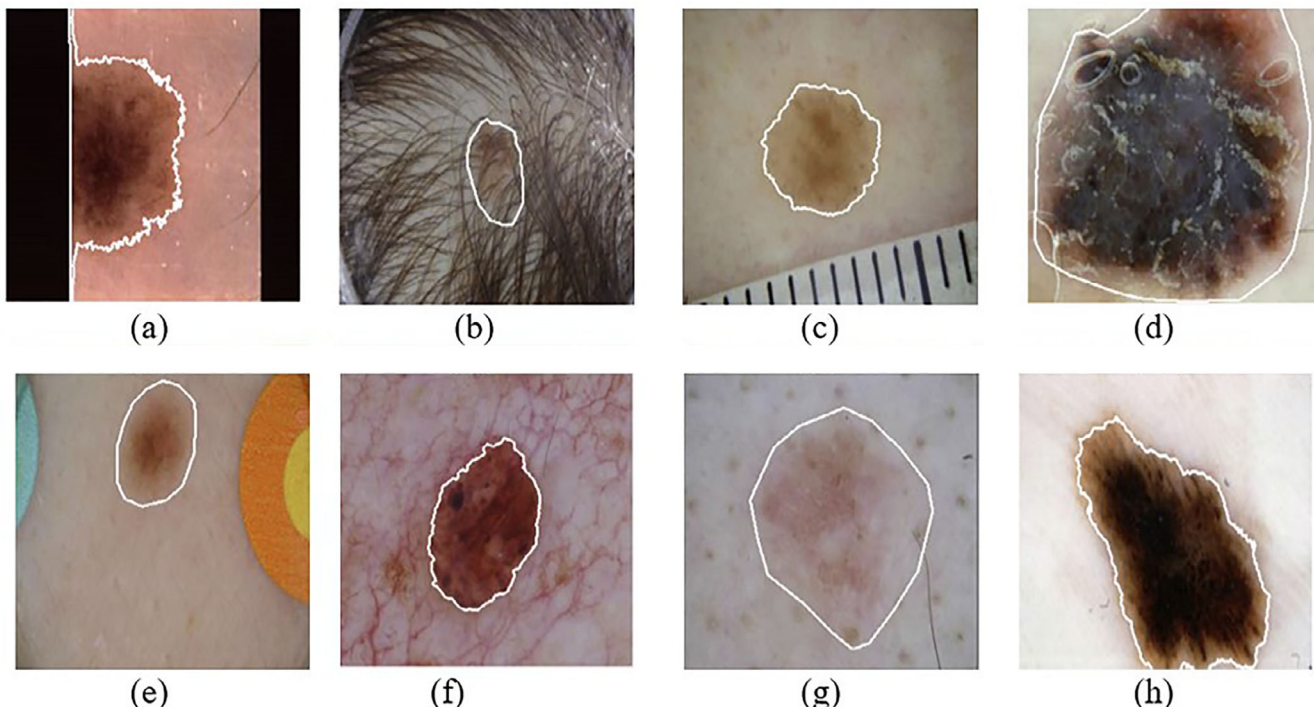


FIGURE 1 Challenges presented in skin lesions. (a) Frame artefact. (b) Hair artefact. (c) Ruler mark artefact. (d) Bubbles. (e) Colour illumination. (f) Blood vessels. (g) Low contrast. (h) Irregular fuzzy rule

reckon the new brightness values. Individuals can use the Wavelet filter control to selectively highlight or de-emphasize details of the image in a particular geographical frequency response. It's equivalent to a stereo's graphic equalizer, except it appears to work on images. Further, these filters also retain the edge and contour information in good shape. However, perfect elimination of all sorts of noise is not possible with these filtering techniques.

In (Sharma et al., 2020) authors performed detailed survey of various hair removal methodologies and discussed about all the problems presented in classification operation if the hair region is presented in the dermoscopy images. They explored that "the skin lesion was imperfectly segmented, and hair based unwanted-improper features are extracted and resulting in the improper classification of diseases". In (Toossi et al., 2013) authors utilized the basic versions of adaptive canny edge detection for segmenting the dark and light hairs. Then, coherence transport inpainting (CTI) approach is used to remove the hairs using multi-resolutions. This (Samuel & Kanna, 2018) method is suitable for the grey scale images only. In (Bibiloni et al., 2017) authors developed the colour morphological process to segment the hair with curvilinear object detection (CUOD). Then, inpainting approach is developed with morphological operations to remove the hair. The main limitation of this approach is that the hair content was removed but they resulted the considerable traces on the skin lesion. In Salido and Ruiz Jr (2017) authors utilized the basic versions filters to remove the noise from skin lesions. They used bottom hat, median filtering with colour space conversion, morphological opening, closing with small-connected pixels identification. Then, harmonic inpainting (HI) approach is used to restore the skin lesions. The different versions of poison noise and random noise were still presented in the skin lesions. To optimize the problems of the filtering approaches, in (Kang et al., 2018) authors used the flow guided filter with curved edge flow (FGF-CEF). Here, they adopted the edge detection method for identifying the angles of hairs region with considerable width. Edge detection is an image recognition method used to detect points in a captured file which have singularities, or sharp modifications in brightness values. The image's corners are the points in which the brightness of the picture differs strongly. Then, finally texture synthesis approach was used along with the curvature edges to restore the hair. This method was suffering with the imperfect analysis of curvatures. It means, the lines presented in the skin dermoscopy images also considered as hair and removed the important disease effected skin tissues. In Khan and Adil (2020) authors developed the morphological based black-hat filtering (BHF) for pre-processing the skin lesions. Then, active counter approach is used along with the Inpainting process to remove the hair region. This method was suffered with the improper classification and segmentation issues due to inaccurate and improper hair removal operation. In (Sau et al., 2018) authors used the contrast adjustment, normalization, anisotropic diffusion filter (ADF) along with calculation of gradient thresholding parameter through sigmoid function. The method was unable to remove the hair content due to over enhancements. The conventional approaches were performed the varies experiments on the random datasets, they are not utilized the anyone of the ISIC dataset. To overcome these problems, in (Talavera-Martinez et al., 2020) authors utilized the DL approaches for detection of hair from skin lesions. The major drawback of this approach is that it utilized the normal skin lesions, then they performed the manual hair simulation. Then DLCNN approach was used to remove this hair content. Only, few experiments were conducted on the real-time hair images. Thus, even though it is an artificial intelligence approach, this method suffers for natural hair images and unable to remove the perfect hair from skin lesions.

Consequently, the following literature survey is focused on various segmentation approaches for detecting the skin lesion. Initially, the various types of thresholding operations (Rahmat et al., 2016) were used to segment the skin lesion. The different types of thresholding methods are Otsu thresholding, simple thresholding, global thresholding, variable thresholding, and multiple thresholding. The (Zhang, 2017) segmentation methods were generated binary map, then by performing the matrix multiplication between binary map to the test image resulted in segmented outcome. But these methods are suffering with the improper skin lesion boundaries. In (Zortea et al., 2017) authors introduced the radial search method to obtain the segmented lesion region from dermoscopy images. The (Sekaran, 2019) thresholding method is applied in the segmentation process and finds the edge using the radial search process. The radial search approach is called a semi-automatic method and, but the major drawback of this approach is that it required the maximum time for initialization and more computational complex. In (Xie et al., 2019) authors utilized the k-means clustering algorithm for identification of skin lesions. The major problem presented in this algorithm was improper selection of k-neighbours. By selecting the average number of clusters, improper area of localization was achieved. In (Nida et al., 2019) authors utilized the fuzzy c-means (FCM) clustering for skin lesion segmentation. Fuzzy clustering is a type of cluster formation that each data item can be assigned to different clusters. Clustering, also known as clustering algorithms, is the method of allocating pieces of data to clusters in a way that items in same cluster are as comparable, whereas items in various clusters are as dissimilar as possible. But this method suffered with the noise sensitivity and initialization of number of clusters. The data are not grouping perfectly and resulted in the imperfect segmentation. In (Soomro et al., 2019), (Hawas et al., 2020) authors used the hybrid approaches of k-means, FCM with modifying their kernel function. Thus, they introduced Gaussian kernels, mean shift kernels, FCM with genetic algorithm, FCM with ant colony optimization (Sengupta et al., 2020), FCM with artificial bee colony, FCM with harmony search algorithm. These bio-inspired optimization algorithms make the system more computational complicated and segmentation of skin lesion also not accurate. Another major drawback of these approaches was, they were not suitable for multiple modalities of skin lesions.

Thus, DL-based segmentation approaches were used to overcome these problems. In (Sengupta et al., 2020), authors used the deep convolutional-deconvolutional neural networks (CDNN) for segmentation of skin lesion on ISIC-2017 challenge dataset. They achieved the first rank in the ISIC-2017 challenge. The main drawback of this approach was training loss is not considered. So, the network was not fully trained

some important features of the skin lesions were eliminated. So, the segmentation performance was not achieved maximum. In (Li et al., 2018) authors used the fully convolutional residual networks (FCRN) for skin lesion segmentation and achieved the second rank in task-2 of the ISIC-2017 challenge. The major problem of this approach is it extracting low-level features for segmentation operation. In (Bi et al., 2017), authors used the Deep Residual Networks (ResNet) for skin lesion segmentation and achieved the third rank in task-2 of the ISIC-2017 challenge. The major drawback of this approach was that the training loss was not calculated, and it is not optimized. The above three literatures are focused on ISIC-2017 challenge and then the following three literatures are focused on ISIC-2018 challenge (Bissoto et al., 2018).

In (Zou et al., 2018), authors developed the pyramid scene parsing network (PSPNet) DL architecture for segmentation. The major drawback of this approach improper pyramidal level weight distribution in the neural networks, resulted in reduction of segmentation accuracy. In (Hardie et al., 2018), authors developed the deep transfer learning (DTL) based ensemble models namely MobileNet, DenseNet-121, and ResNet50 for segmentation process. The major drawback of this approach was the models not perfectly synchronized and optimization also not performed. In (Abraham & Khan, 2019) authors utilized the U-Net based DL segmentation with Tversky index-based network loss optimization. Here, they used Tversky index for improving the system performance, but it resulted reduction of system speed. Thus, to overcome these drawbacks, this article was utilized the block-based DL architecture with loss analysis for effective segmentation.

The following survey focused on various types of feature extraction mechanisms. The effective classification operation can be performed through the accurate feature extraction only. The cancer classification majorly depended on asymmetry, border, colour, diameter, and edge (ABCDE) properties. Thus, the extracted features must inhabit this ABCDE properties. Thus, the in conventional various works (Chatterjee et al., 2019) focused on extracting the low, medium, and high-level features by using image processing methods. The different intensity, texture-based features are extracted from the segmented image then the Haralick features were formed. Then, the authors (Chatterjee et al., 2019), (Alfed & Khelifi, 2017) utilized the grey level co-occurrence matrix, discrete wavelet transform and local binary pattern-based approaches and various transforms for feature extraction process.

The major drawback of these approaches was the features need to be optimized, because all the extracted features were not accurate. Thus, to overcome these problems again feature selection methods are introduced. These features select the optimal features from the set features such as the texture, shape, colour, and other spectral features. Analysing the various feature selection methods such as information gain, gain ratio, best-first search algorithm, chi-square test, recursive feature elimination processes were used in the conventional mechanisms (Tan et al., 2018) Anyhow, ABCDE property of the features are eliminated by selecting the only few features from images. Finally, DL (Amin et al., 2020) based mechanisms are introducing to extract the optimal features from each pixel of segmented skin lesion. But the conventional DL approaches does not have the separate models for differentiating disease dependent and disease specific features. The proposed model is designed to detect the skin cancer and classification using FrCN based deep learning convolutional neural network (CNN) with transfer learning. It helps in denoising model of skin lesions for Benign tumours grow slowly and rarely spread. Malignant tumours can spread throughout the body, penetrate and destroy near the area normal tissues, and grow quickly inpainting the procedure. Thus, the conventional DL models have the considerable problem with subtypes of benign and melanoma skin cancer features. Specific target cancer drugs, immunotherapeutic, radiation treatment, or chemotherapy could sometimes aid shrink a melanoma, reduce the severity, and feel better. Other treatment options are able to treat symptoms are the steps to control the melanoma effects.

Finally, following literature survey focused on classification various machine and DL methods. Initially, the machine learning approaches such as support vector machine (Bakay & Ağbulut, 2021) random forest (Li et al., 2018), Navie Bayes (Balaji et al., 2020) were widely used for classification purposes. But these methods gave better results for only small datasets and not useful for the ISIC challenge datasets. Thus, the DL-based approaches like artificial neural networks (ANN), Back-propagated-ANN (Hekler et al., 2019) DenseNet 201 (Guissoos, 2019) CNN with data augmentation (CNN-DG) (Sun et al., 2021) DLCNN (Mohamed & El-Behaidy, 2019) and Multi-scale Multi network-based CNN (MCM-CNN) (Mahbod et al., 2020) for the classification of skin lesions. In (Nozdryn-Plotnicki et al., 2018) authors used the utilized the transfer learning based ensembled CNN (ECNN) for classification of skin cancer and achieved the first rank in ISIC-2018 sub challenge. In (Gessert et al., 2018) authors used the ResNeXt, SENet and DenseNet (RSD) models with batch normalization-based weight loss optimization. This work achieved the second rank in the in ISIC-2018 challenge and achieved the first rank in ISIC-2019 challenge. The major drawback of this approaches is that it can detect the only few diseases and if the number of layers is increased then the computational complexity was increased with huge training loss and consuming the more time for network training. Thus, to overcome all these problems, this article is contributed as follows:

1. Initially, HGF-CCL based fast march inpainting is used to remove the hair and noise. Then, FrCN segmentation approach is utilized for identifying the skin lesions.
2. The DRB based DLCNN architecture is used to extract the features with disease dependent and disease specific properties.
3. Then, Transfer learning based three separate models are used to perform the eight-class classification operation.
4. The experiments are carried out on ISIC 2019 challenge dataset with eight class diseases, they are squamous cell carcinoma (SCC), vascular lesion (VASC), dermatofibroma (DF), benign keratosis (BKL), actinic keratosis (AKIES), basal cell carcinoma (BCC), melanocytic nevus (NV), and melanoma (MEL).

Rest of the article is organized as follows: Section 2 deals with the detailed analysis of the proposed method with DL models. Section 3 performs the detailed analysis of simulation and comparison with state of art approaches. Finally, Section 4 concludes the article with possible future enhancements.

The article is structured as follows.

The section one is described as Proposed methodology, the section two give the segmentation training loss analysis, the section three describe about dataset, the forth section is filtering and hair removal, the fifth section is conclusion.

2 | PROPOSED METHODOLOGY

The proposed model skin cancer detection and classification model is presented in Figure 2. It gives the detailed operation of preprocessing, hair removal, FrCN segmentation, DLCNN feature extraction and transfer learning-based classification, respectively. The complete algorithm of the proposed model is presented in Table 1.

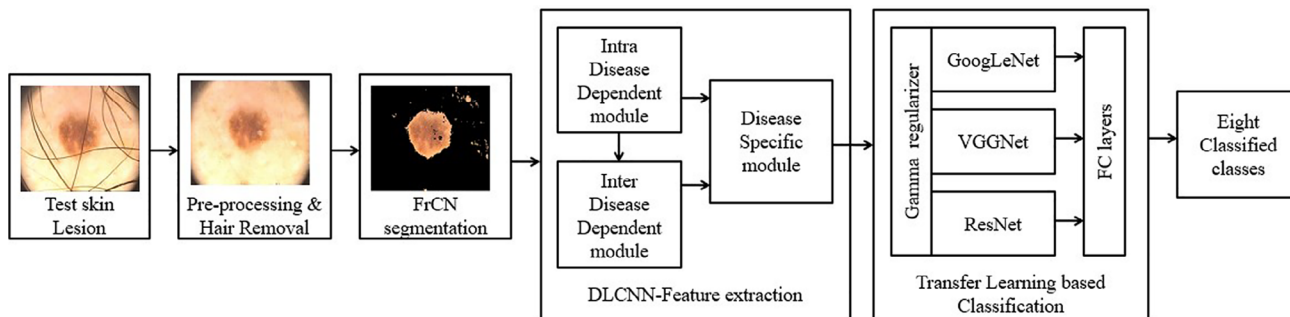


FIGURE 2 Proposed FrCN-based DLCNN with transfer learning for skin lesion segmentation and classification

TABLE 1 Algorithm of proposed segmentation and classification model for skin lesion diagnosis

| |
|-----------------------------------------------------------------------------------------------------------------------------------------------------------------------------------------------------------------------------------------------------------------------------------------------------------------------------------------------------------------------------------------------------------------------------------------------------------------|
| Input: Test skin lesion |
| Output: Type of disease classified |
| Intermediate outcomes: hair removal outcome, segmented skin lesion |
| Objective evaluation- set 1: PSNR-HVS, PSNR-HVS-M, MSSSIM, UQI, VIF, RMSE, MSE, PSNR, SSIM |
| Objective evaluation- set 2: SEN, SPE, ACC, DIC, JAC, MCC of segmentation |
| Objective evaluation- set 3: Accuracy, AUC, Sensitivity, Specificity, precision of feature extraction |
| Objective evaluation- set 4: Accuracy, AUC, Sensitivity, Specificity, precision of classification |
| Step 1: Perform the training operation on various deep and transfer learning models using ISIC-2019 dataset. |
| Step 2: Perform HGF-CCL based Fast March inpainting procedure for hair and noise removal on test skin lesions. |
| Step 3: Perform the FrCN segmentation operation on hair removed outcome. |
| Step 4: Extract the diseases specific and disease dependent features by using DLCNN. |
| <ul style="list-style-type: none"> • Inter-DDM based DRB is used to extract the disease dependent or differentiate the features of benign and melanoma separately. • Intra-DDM based DRB is used to extract the within the similar disease dependent features or sub-types of disease dependent features of benign and melanoma. • The specific relationship between each disease is identified by using the DSM based DRB. |
| Step 5: Perform the classification operation using Transfer learning models with above features. |
| <ul style="list-style-type: none"> • VGGNet is used to generate the probabilities of AKIES and BKL diseases. • GoogLeNet is used to generate the probabilities of MEL, NV, and BCC diseases. • VGGNet is used to generate the probabilities of DF, VASC, and SCC diseases. • The system is optimized by the Gamma regularizer. • Then fully connected layers are used to classify the eight disease classes. |
| Step 6: Perform the subjective and objective evaluation. |
| <ul style="list-style-type: none"> • HGF-CCL based Hair and noise removal process results the objective evaluation of set-1. • FrCN based segmentation process results the objective evaluation of set 2. • DRB based feature extraction results the objective evaluation of set 3. • Transferring learning model base classification results the objective evaluation of set 4. |

2.1 | Filtering and hair removal model

Figure 3 presents the novel method for hair and noise removal approach using HGF-CCL based fast marching inpainting procedure. Inpainting is a conservation technique which fills in damaged, deteriorating, or lacking sections of an artwork to create a complete image. This method could be used on both physical and virtual forms of art, such as petroleum or paint paintings, chemical photographic prints, artworks, or digital photos and video. The suggested method consists of two operations, which includes the detection and removal of hair, and the potential to eliminate the additional noise components to enhance the skin lesion image quality. Skin lesions are regions of skin which vary from the surrounding region in looks. They are commonly bumps or patches, but they can be affected by a range of issues. A skin lesion is defined by the United States Society for Dermatologic Surgery as an abnormal lump, knock, ulcer, sore, or different coloured area of the skin. Consider the original image O_{ij} and it is affected by Gaussian noise G_{ij} with i^{th} row, and j^{th} column pixel values. Then, the resultant noisy image X_{ij} is given as below:

$$X_{ij} = O_{ij} + G_{ij} \quad (1)$$

Here, Gaussian noise is a zero-mean noise, thus SD plays significant role in the process of elimination of all noises. Generally, the SD is used to change the window size automatically in the filtering process. Gaussian noise, named after Carl Friedrich Gauss, is statistical with same probability density function as the normally distributed, also recognized as the Gaussian distribution. This motivates us to develop the HGF approach, which utilizes the variable convolution mask for precise estimation of Gaussian noise variance in X_{ij} . This mask is then convolved with the X_{ij} . Here, the Gaussian mask generation purely depends on the eigen threshold values, which is used to eliminate the Gaussian noise. Threshold operations. The significance level is measured during the arranging of an A/B test as well as relates to the probability of committing a type I error that is considered appropriate under particular circumstances of the test throughout question. Usually, the Gaussian thresholding will be performed at the transform level not in the spatial level. The Gaussian smoothing operator is a 2-D permutation operator used it to blur images by discarding detail and loud sounds. It is related to the average filter in this respect, but it utilizes a different kernel that reflects the shape of a Gaussian hump. Thus, the good pixels are perfectly selected by the thresholding process.

Table 2 demonstrates the algorithm of proposed HGF-CCL based fast marching inpainting process for the detection and removal of hair from the obtained denoised outcome using HGF algorithm presented in Table 3.

2.2 | Segmentation model

Normally, some important features of specific pixels will be losses due to decoding, deconvolution, convolution, bilinear interpolation, up-down sampling, and reduced image size in segmentation operation. Thus, these missing pixels and features are effectively restored by using the advanced DL approaches. Along with DLCNN architectures, conditional random field (CRF) and parallel integration (PI) methods are used for further improve the segmented boundaries or edges. This article presents the FrCN based DL architecture, it is used to perform the segmentation operation. The DL architecture of segmentation method using FrCN is presented in Figure 4. The FrCN network is developed from the inspiration of VGG-16 network and it contains 16 layers. A segmentation model is a physical tool which can be formed in a spreadsheet program which delivers calculations and standings for recognized important components required to meet your purposes within a particular segment. The last three fully connected layers of VGG-16 was replaced by convolutional and dropout layers in the FrCN network. Table 4 presents the sizes of various convolutional layers along with feature maps and filters for each block. The FrCN based CNN model consisting of two important parts for accurate pixel-wise segmentation. The first part of the segmentation network consisting of sub-sampling and convolutional layers. Subsampling is

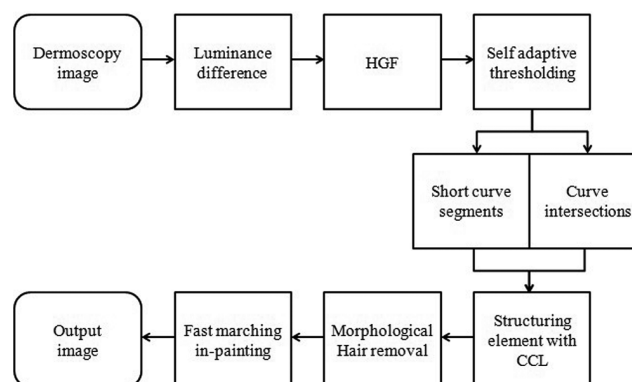


FIGURE 3 Block diagram of proposed HGF-CCL based fast marching inpainting process

TABLE 2 Algorithm of proposed HGF-CCL based fast marching inpainting process

Input: Test skin lesion.
Output: Hair and noise removed skin lesion.

Step 1: Read the hair containing colour input dermoscopy image.

Step 2: Convert the input image into LUV colour space and compute the brightness difference for quick emphasizing of hair content in the dermoscopic image.

Step 3: Apply HGF filtering (refer Table 2) to eliminate noise components while preserving the original information.

Step 4: Apply the self-adaptive thresholding operation for detection of hairs so, the background of the hair (skin lesion) is perfectly identified.

Step 5: Apply CCL procedure. It divides the skin lesion as follows:

- The curved intersections with the line angles are used to detect the corners.
- The short curve segments were used to detect the hair end to end points.
- The intersection analysis was also used to determine the edges and thickness.

Step 6: Use structuring elements to apply the morphological image close procedure.

- Each connected label component's area is calculated.
- It removes all labelled objects with a pixel count of less than 50.
- To filter out small things, use the morphological area opening operation.

Step 7: The morphologically created hair removal mask is multiplied with a test colour skin lesion.

Step 8: Finally, fast marching in-painting procedure is applied to remove the small parts of hair, restores and refines the skin lesion. The Fast-Marching Method recommends an Eikonal formula solution for a regular grid, where velocity attributes at each point demonstrate the refractive index. The function for wave expansion is denoted by this artificial refractive index.

TABLE 3 HGF algorithm

Input: noisy image X_{ij}
Output: Denoised image Y_{ij}

Step 1: Read input noisy image (X_{ij}) which has the size of $M \times N$.

Step 2: Calculate the SD of Gaussian noise (σ_{GN}) through the input convolution with Gaussian mask as given below:

$$\sigma_{GN} = \frac{1}{MN} \sum_{i=1}^M \sum_{j=1}^N |X * MASK|_{ij} \quad (2)$$

Here, $*$ indicates convolution process.

Step 3: Now, choose the size of Gaussian window reckon on σ_{GN} .

$$w = \begin{cases} 3 \times 3, \sigma_{GN} < 20 \\ 5 \times 5, \sigma_{GN} \geq 20 \end{cases} \quad (3)$$

The selection of Gaussian window plays the significant role in the noise elimination process. Usually, the lesser window size such as 3×3 is selected for the elimination of low-level noises and preserves the perfect edges. Then, the higher window size such as 5×5 is selected for the elimination of high-level noises and restores both spatial and texture region. Thus, various noise levels are eliminated by distinct window sizes, and the computational complexity can also be significantly reduced as compared to the unchanged size windows.

Step 4: Execute the operation of mean filtering on X_{ij} using the chosen size of window.

$$\tilde{X}_{ij} = \frac{1}{R} \sum_{i=1}^R \sum_{j=1}^R X_{ij} * w_{ij} \quad (4)$$

Here, R indicates the total number of pixels presented in the local mask, which is usually 9 or 25

Step 5: Now, apply the sliding window on X_{ij} , so the window mask can be moved and mean of total patches are calculated. Compute the absolute difference between X_{ij} and \tilde{X}_{ij}

$$D_{ij} = |X_{ij} - \tilde{X}_{ij}| \quad (5)$$

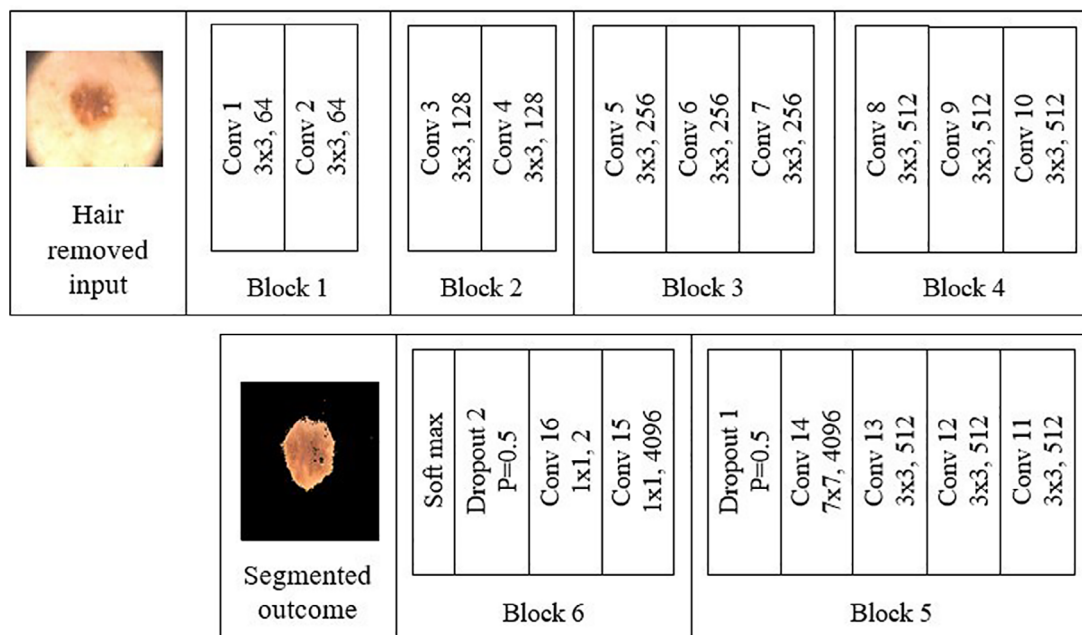
Step 6: Selection of pixels based on the absolute mean μ . For low level μ values, the resultant data V is selected as difference data D_{ij} and for high level μ values, the resultant data V is selected as mean data \tilde{X}_{ij} .

$$V = \begin{cases} \{D_{(1)}, D_{(2)}, D_{(3)} \dots D_{(n)}\}, D_{ij} < \mu \\ \{\tilde{X}_1, \tilde{X}_2, \tilde{X}_3, \dots, \tilde{X}_n\}, D_{ij} \geq \mu \end{cases} \quad (6)$$

Step 7: Calculate the mean of vector V and it resulted the denoised outcome Y_{ij} as follows

$$Y_{ij} = \text{mean}(V) \quad (7)$$

a technique for reducing size of the data by having removed a subset of the original data. Convolutional layers are the main components of convolutional neural networks. A convolution is generally a function of a filter to an input, that results in activation. As a result, extremely specialized features which can be identified anywhere on input images are generated. The test input images are applied to the convolutional layers, these layers are utilized to extract the deep features from test images by using the different types of filters with various kernel sizes. Then, the extracted

**FIGURE 4** Proposed FrCN segmentation method**TABLE 4** Proposed FrCN layers information

| Block | Layer | Filter size, maps | Block | Layer | Filter size, maps |
|------------|---------|-------------------|-------|-----------|---------------------------|
| Input data | | — | | Conv 11 | $3 \times 3, 512$ |
| Block-1 | Conv 1 | $3 \times 3, 64$ | | Conv 12 | $3 \times 3, 512$ |
| | Conv 2 | $3 \times 3, 64$ | | Conv 13 | $3 \times 3, 512$ |
| Block-2 | Conv 3 | $3 \times 3, 128$ | | Conv 14 | $7 \times 7, 4096$ |
| | Conv 4 | $3 \times 3, 128$ | | Dropout 1 | $P = 0.5$ |
| Block-3 | Conv 5 | $3 \times 3, 256$ | | Conv 15 | $1 \times 1, 4096$ |
| | Conv 6 | $3 \times 3, 256$ | | Dropout 2 | $P = 0.5$ |
| | Conv 7 | $3 \times 3, 256$ | | Conv 16 | $1 \times 1, 2$ |
| Block-4 | Conv 8 | $3 \times 3, 512$ | | Soft-max | — |
| | Conv 9 | $3 \times 3, 512$ | | | $192 \times 256 \times 3$ |
| | Conv 10 | $3 \times 3, 512$ | | | |

feature maps sizes are reduced by using the sub-sampling layers. These layers will reduce the feature over fitting and eliminates the unwanted redundancy features, thus the time complexity is minimized. The second part of the network consisting of up-sampling layers and soft-max layer. The up-sampling layers improve feature spatial redundancy and temporal redundancy. Thus, the appropriate pixel information is obtained. Then, the soft-max layer acts as classifier and it is used to identify the effected lesion region and normal tissue region through the classification process.

The detailed procedure of segmentation procedure is explained as follows:

- The basic features are extracted by using the convolutional layers from test image each pixel. The block-based convolution network generates the accurate feature maps (F) with various sizes through the different filters. The feature maps are calculated as follows:

$$F_L^k = \emptyset(W_L^k * F_{L-1}^k + b_L^k) \quad (8)$$

- Here, L indicates the Layer number, k indicates the feature maps. The fundamental elements of the FrCN network are activation function $\emptyset(\bullet)$, filter kernels (W), bias function (b_L^k) and convolution operator (*). Here all these operations are performed on each layer with each feature map.

- The rectified linear unit (ReLU) activation function gives the higher efficiency with lower computational complexity in the training procedure as compared to the conventional sigmoid and tan h functions. Here, the ReLU based nonlinear activation function is used after every convolutional layer, thus the non-linearity of the FrCN network is achieved and reduces the vanishing gradient problems. Non-linear functions fix the issues connected with activation functions. They enable the stacking of numerous layers in the neural to create a deep convolutional neural network. Finally, the mathematical operation of ReLU is given as follows:

$$\phi(x) = \max(0, x) = \begin{cases} x, & \text{if } x \geq 0 \\ 0, & \text{if } x < 0 \end{cases} \quad (9)$$

During the training process, Dropout removes the unnecessary units with its interconnections. Thus, the overfitting problems presented in the deep layers can be effectively removed. Specifically, after 14th and 15th convolutional layers, the FrCN network contains the dropout with probability $P = 0.5$. Hence, every unit is retrained with the $P = 0.5$ probability.

Finally, The SoftMax classifier is used to classify the lesion, skin pixels and exact segmentation operation is performed. The SoftMax classifier is a multinomial logistic regression model, thus the multi-modality of pixels is perfectly analysed. Hence, the lesion predictions of each pixel and generates the segmented map without changing the resolution of test image.

2.2.1 | Segmentation training loss analysis

During the testing and training phase of pixel- wise classification of skin lesions in the segmentation process, the cross-entropy loss function is utilized in the FrCN for analysing the total loss of neural networks. The total loss (H) of each pixel is reduced by estimating the cross-entropy loss among the predicted segmented map (\hat{y}) and ground truth annotation (y), respectively. The total loss is defined as follows

$$H = -(y \cdot \log(\hat{y}) + (1 - y) \cdot \log(1 - \hat{y})) \quad (10)$$

By calculating loss function, the weights of each layer in the FrCN can readjusted, so better segmentation accuracy can achieve. To get the optimal performance, initially the weights in output layers calculated sequentially during the training phase. Then, the error between weights of ground truth and predicted labels are calculated by using the total loss (H) across the final output layer. To reduce this error, the weights are re-applied to the intermediate layers in the back-propagation manner. The weight updatation process repeats until the optimal performance of the FrCN network obtain.

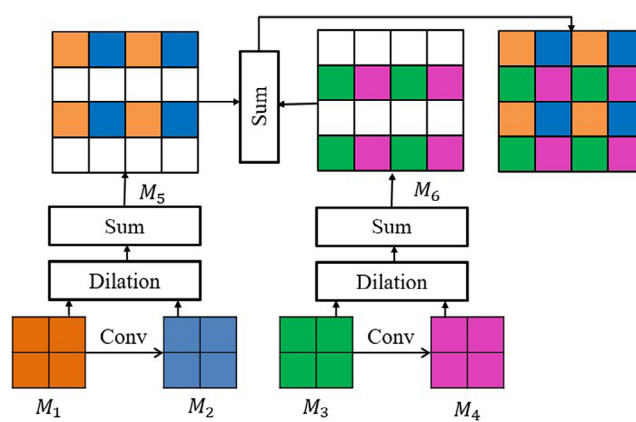
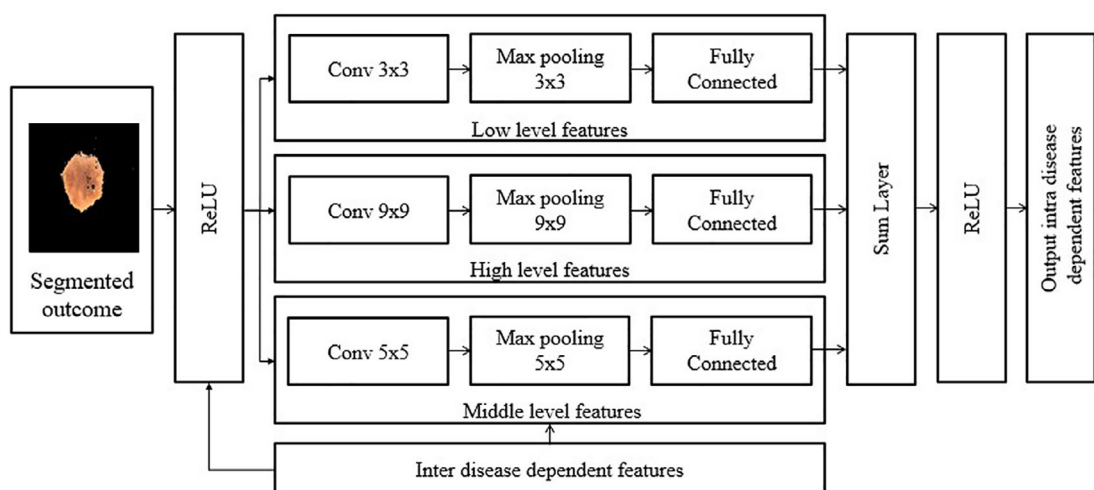
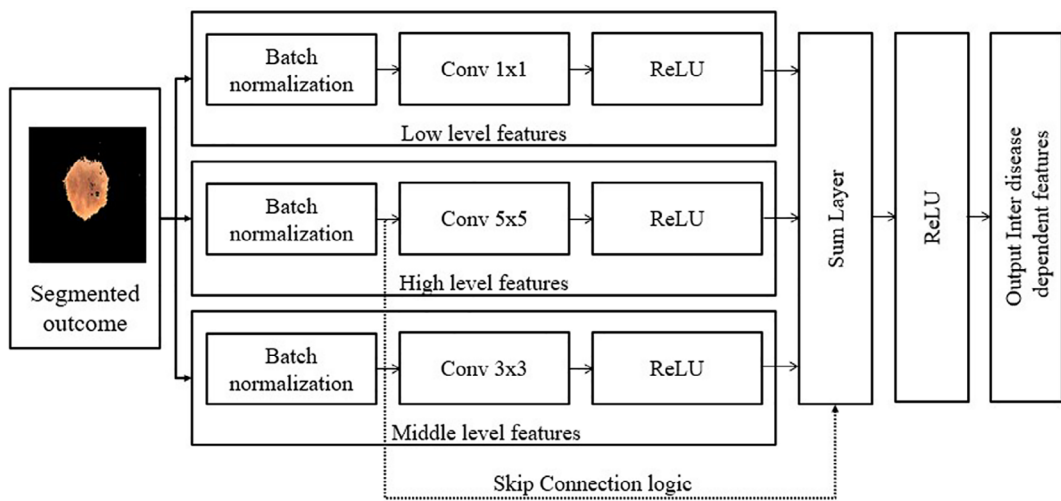
2.3 | Deep feature extraction model

After the segmentation process, the DLCNN based RefineNet is used for the feature extraction of the segmented skin lesion. The DLCNN utilizes the multiple convolutional layers to extract the hierarchical features. Each disease has its own features, so it is necessary to calculate dependency and relationship between eight diseases. The classification accuracy can improve significantly by extracting the accurate features. The proposed DLCNN consisting mainly three modules as shown in Figures 5, 6 and 7, respectively. They are inter- disease dependent module (Inter-DDM), intra disease dependent module (intra-DDM) and disease specific module (DSM), respectively. Here, the intra-DDM and inter-DDM are used to identify the dependency between eight diseases. These three modules are developed by using the four deep residual blocks (DRBs) with various filter sizes and feature maps. Multi-scale output features are generated by using various sizes of the feature maps.

Initially segmented skin lesion is applied to the Inter-DDM based DRB. The inter-DDM is used to identify the relationship between benign and melanoma and restores the complete dependency of features by using up sampling. Thus, two major types of disease features are extracted. Then output features of the inter DDM-DRB are applied as input to the intra-DDM based DRB, respectively. Here, intra-DDM is specifically designed to identify the relationship within the various subtypes of benign and melanoma and extracts the semantic features by using down sampling. After calculating the dependency between eight diseases, the specific feature of eight diseases is calculated by using the DSM based DRB.

2.3.1 | Inter-DDM based DRB

This module is used to extract the high-level, middle-level, and low-level based disease dependent hierarchical features on each pixel of skin lesion as shown in Figure 6. Thus, two major types of disease features are extracted. The feature extraction performance is depending on the number of layers presented in the DRB. The segmented skin lesion is applied as input to batch normalization layer of DRB.



The batch normalization reduces the effects of unstable gradient features. Instead of large convolution layers, convolution layer with 1×1 kernel is used after the batch normalization layer. Thus, the number of convolutional parameters is reduced, and overfitting problem also avoided. Then, ReLU activation function is used to identify the inter dependency of features. The rectified linear activation function, simplified ReLU, is a piece-wise linear that produces an output the inputs if it is optimistic or else, it generates zero. This first level extracts the low-level features. Like this, another two levels of Batch normalization with 5×5 convolution layer and 3×3 convolution layer is used for high-level and middle-level feature extraction. Finally, all these features are fused by using the sum layer. Finally, output feature map is generated by the applying the ReLU activation function on the fused feature map.

2.3.2 | Intra-DDM based DRB

The output feature maps of Inter-DDM based DRB are applied as input to the Intra-DDM based DRB for each max-pooling layer as shown in Figure 7. So, individual disease specific features are extracted detailly with maximum information. The segmented skin lesion is also applied as input to ReLU activation function of DRB. Here, the segmented input pixels basic disease specific features are selected through Inter-DDM based DRB outcomes by ReLU activations. This DSM based DRB contains the three levels of convolutional layers, and max-pooling layers. These three levels are used to extract the low, middle, and high disease dependence features. Convolutional layers are used to extract the initial hierarchical features through $\{3 \times 3, 5 \times 5$, and $9 \times 9\}$ sized kernel matrix. The convolutional feature maps size is increased by using the max-pooling layer with $\{3 \times 3, 5 \times 5$, and $9 \times 9\}$ feature size and it also boost the performance by leveraging global contextual data. The total captured within disease dependent features are increased by increasing the size of the max-pooling layer and achieved the more robust performance against various translations. Finally, output feature map is generated by the performing the fusion operation on three level feature maps.

2.3.3 | DSM based DRB

This module is mainly responsible for identifying the specific relationship between various diseases and the various intra and inter dependent features are separated based on their relationship by using the dilated convolution operation. Finally, this module is also responsible to fuse the multi-level intra and inter dependent features. Both the inter-DDM and intra-DDM features are applied as input to the DSM based DRB as shown in Figure 7. Consider, M_1, M_2 be the first feature maps of inter-DDM, intra-DDM and M_3, M_4 as the second feature maps of inter-DDM, intra-DDM. Initially, the interleaving operation is performed between M_1, M_2 and M_3, M_4 individually. Thus, the features maps interleaves with various kernel weights from zero to the 8×8 size, respectively. Here, the dilated convolution is used to perform this interleaving operation. These two resultant dilated feature maps are added together and generates the final output feature map.

2.3.4 | Feature extraction loss analysis

The feature extraction performance is increased by increasing the number of layers in the DLCNN; thus, the more hierarchical features are extracted from the segmented skin-lesion. But the exploding or gradient vanishing problems are generated by using a greater number of layers and it results in more complicated training process. By using the skip connection, the shortest path will be established from the input to the output in the back propagation manner. The gradients are effectively transferred to the lower layers by the skip connection through the back propagation manner. These problems are effectively solved by using the skip connection. Thus, number of computations and checkerboard issues are reduced during the training the process for similar pixels. Consequently, the parameters of kernels and feature maps of the network also remains maintained same by using this skip function logic. As a result, the relationship between various features also significantly improves by this back propagation. The disease specific features efficiency is improved by increasing the max-pooling efficiency through the non-linear ReLU operation.

The operation of back propagation-based skip connection is illustrated as follows:

$$h_{l+1} = \text{Relu}(h_l + \mathcal{F}(h_l, \omega_l)) \quad (11)$$

Here, the rectified linear unit activation function is indicated by $\text{Relu}()$, residual mapping function denoted as $\mathcal{F}()$, h_l represents the input layer, h_{l+1} represents the output layer and ω_l represents the weight coefficients of l -th layer, respectively. The gradient derivatives are generated in the back propagation mechanism are illustrated as follows

$$h_L = h_l + \sum_{i=1}^{L-1} \mathcal{F}_i(h_i, \omega_i) \quad (12)$$

$$\frac{\partial \mathcal{L}}{\partial \mathbf{h}_l} = \frac{\partial \mathcal{L}}{\partial \mathbf{h}_{\mathcal{L}}} \cdot \frac{\partial \mathbf{h}_{\mathcal{L}}}{\partial \mathbf{h}_l} = \frac{\partial \mathcal{L}}{\partial \mathbf{h}_{\mathcal{L}}} \left(1 + \frac{\partial}{\partial \mathbf{h}_{\mathcal{L}}} \sum_{i=1}^{\mathcal{L}-1} \mathcal{F}_i(\mathbf{h}_i, \omega_i) \right) \quad (13)$$

From the above equations, it is observed that the gradients can be easily pass from one layer and another layer though the skip connection. The over fitting and gradient vanishing problems are effectively solved by controlling the training loss and initialization operations, respectively. Here, total loss function is indicated by the \mathcal{L} and it is calculated as follows:

$$\mathcal{L} = \sum_{s,m} \omega_s \cdot \mathcal{L}_s + \omega_m \cdot \mathcal{L}_m \quad (14)$$

Here the predicted output or side output loss function is indicated by \mathcal{L}_s and main output loss value is indicated by \mathcal{L}_m . Finally, the weight coefficients of loss layers are denoted by ω_m and ω_s .

2.4 | Classification model

In the practical scenarios, it is exceedingly difficult to perform the training operation of eight classes by using DLCNN models. The resultant feature map from the DLCNN architecture is applied to the transfer learning model for the classification of skin cancer. Thus, the test image is not matched with the anyone of eight classes or it results in the improper classification. Thus, to solve this problem, transfer learning methodology has been introduced. It is an efficient classification mechanism of DL. The major operational steps of transfer learning approach are: (a) selection of pre-trained model, (b) problem size, similarity, and (c) classification operation. Here, pre-trained model is used to solve the multiple problems based on the similarity between individual problems. Thus, the multiple problems can be effectively solved by using the constraint optimization approach. It means the solution generated for one problem can be effectively used to solve the other related problems also by using the background knowledge used. Here, the eight types of skin cancers similarity are effectively identified during the testing phase and results the accurate classification operation. This article utilizes VGGNet, ResNet, and GoogLeNet and based three individual transfer learning models for classify the eight disease classes. Here, VGGNet is specifically used to classify the MEL, NV and BCC diseases. Then, GoogLeNet is used to classify the AKIES and BKL diseases. Finally, ResNet is specifically used to classify the DF, VASC and SCC diseases, respectively. This can be achieved by performing the individual training operation of that transfer learning models with the deep residual features of each disease through the transfer learning theory. Finally, fully connected layers are used for combined classification of all diseases.

2.4.1 | VGGNet

This model contains the same network architecture as that of AlexNet and contains extra convolution layers. Figure 8 presents the detailed architecture of VGGNet. Alex Net is an eight-layer deep convolutional neural network. A pre-trained models version of the network trained with over a million pictures from the ImageNet dataset can be loaded. The pretrained network could really classify images into 1000 distinct object categories, such as keyboards, mice, marker pens, and a variety of animal life. VGG Net is a neural network that achieved success in ILSVRC. It came with first place for image localization and second place for image processing. Each year, the ImageNet team organizes an image recognition competition. It contains 3-FC layers and 13-convolution layers, 5-pooling layers, SoftMax classifier. The VGGNet utilizes the 3x3 kernel wind size for convolution network with 2×2 size of pooling network in the seven layered formats. Finally, SoftMax classifier is used to perform the classification operation based on the pre-trained database. Due to this network connections, it gives the better classification of diseases as compared to the AlexNet model.

2.4.2 | GoogLeNet

It is the small network as compared to the VGGNet and AlexNet, thus it is used to classification of only two diseases. Figure 9 presents the detailed architecture of GoogLeNet. This network contains the three 1×1 convolutional layers, 3×3 max pooling with a stride of 1, 3×3

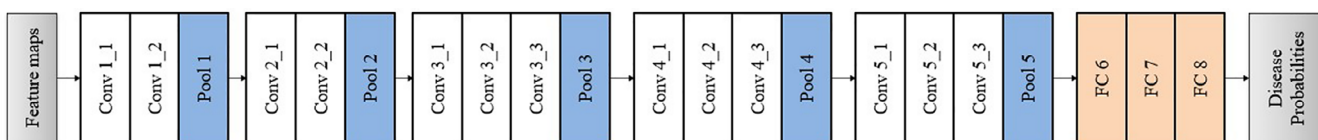


FIGURE 8 Architecture of VGGNet

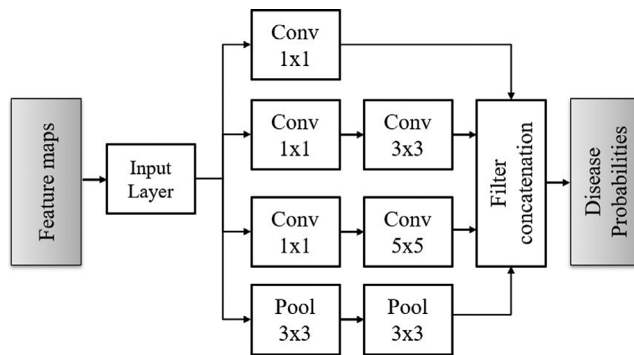


FIGURE 9 Architecture of GoogLeNet

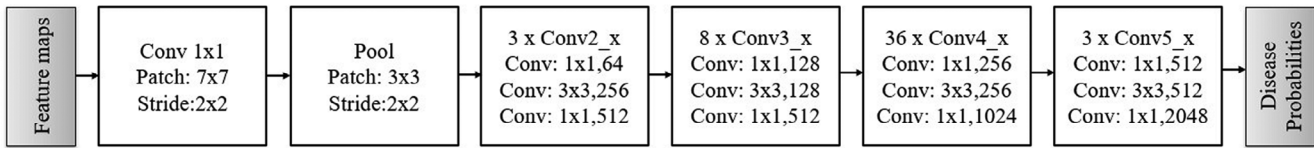


FIGURE 10 Architecture of ResNet

convolution and 5×5 convolution layers. Finally, all the layers are concatenated using filtering approach. Here, convolution layers act as the repeater to the input. Here, these layers utilize the optimal filter sizes and reduces computational complexity and minimizes the number of parameters. Thus, it gives the optimal performance of two class classification.

2.4.3 | ResNet

It is a type of deep residual network and gives the better classification performance for various types of real-time applications. Figure 10 presents the detailed architecture of ResNet, and it is used to classify the three diseases. ResNet consisting of the convolution layers with various filter sizes, thus it results in the reduction of training time along with degradation problem. Finally, it gives the classification output of three diseases.

2.4.4 | Classification loss analysis

This article utilizes the gamma regularizer for reduction of training loss and computational complexity generated in the transferer learning mechanism. This gamma regularizer works based on the classifier weight matrix optimization through SD estimation. Thus, the weight coefficients will maintain similarity. Weighted classification is aimed for classification problems for which achieving a good classifier model for particular classes is crucial. With the most important categories, weighted classification techniques offer simpler designs. Moreover, they do this without affecting the quality of the prediction classifier. so, the correlation between weight coefficients is achieved. The mathematical analysis of gamma regularizer is derived as follows:

$$\lambda \sum_{i=1}^k \sigma(\omega_i) \quad (15)$$

Here, λ is a gamma regularization metric, it updates and corrects the weight coefficient matrix from disperse and large values. Then, ω denotes the filter weight coefficient, number of filters available in convolution layer denoted by k , number of parameters in convolution layer denoted by n and it is based on the resolutions of the filter or kernel. Then, the SD is indicated by the σ and it is calculated as follows:

$$\sigma(\omega) = \sqrt{\frac{1}{n} \left\{ \sum_{i=1}^k \omega_i^2 - \frac{1}{n} \left(\sum_{i=1}^n \omega_i \right)^2 \right\}} \quad (16)$$

3 | RESULTS AND DISCUSSION

This section gives the detailed analysis of the results with both quantitative and quality evaluation. All the experiments are conducted by using MATLAB R2021a simulation platform. The maximum number of training epochs was set to 50 with 0.00001 initial learning rate.

3.1 | Dataset

The publicly available and real time ISIC 2019 challenge dataset is considered for the training and testing of the proposed model. This dataset contains the BCN_20000 and HAM10000 images. Here, the HAM10000 contains the 10,000 images with each image size as 600×450 . The BCN_20000 consisting of 19,424 images with each image size as 1024×1024 . The ISIC dataset contains the total 25,331 images and this dataset is distributed as follows: SCC contains 628 images; VASC is 253, DF is 239; BKL is 2624; AKIEC is 867; BCC is 3323; NV is 12,875 and MEL images is 4522. The entire dataset is categorized into three parts. They are 10% dataset consider for testing, 10% for validation and 80% dataset for training. The DL models are used for segmentation and feature extraction of the skin lesions. The eight-class classification is performed by using transfer learning model.

3.2 | Subjective evaluation

Figure 11 shows performance of the proposed HGF-CCL based hair removal and FrCN based segmentation on eight different types of skin cancer images, respectively. The proposed system perfectly removed hair artefacts and filters the various types of noises. From the figure, it is also observed that the proposed method effectively detected the regions of skin cancers with perfect edges. Change to the DNA inside cells cause cancer. In a cell, DNA is organized into many specific genes, which each includes a sequence of commands notifying the cell what features to perform and how to develop and split. The cancer can be controlled by eating healthy food, should be vaccinated regularly, protect from sun. From the Figure 12, it is observed that the conventional approaches failed to remove the hair accurately from the skin lesions. For example, methods from Goyal et al., (2020); Hardie et al., (2018) literatures were unable to detect the hair, so the segmentation of hairs not performed. Thus, the output images contain the lot of hair content. From the literatures Gutman et al., (2016); Hawas et al., (2020), these methods successfully detect and segments the hair, but the inpainting approach not applied perfectly, thus it resulted in presence of some hair content. The methods presented in Guissous et al., (2019); Khan et al., (2020); Hekler et al., (2019) are removed the entire hair content, but still noises are presented, and some hair traces still presented. Thus, to overcome these drawbacks, the proposed method utilizes the HGF filtering for noise removal, CCL for segmentation of hair and Fast March inpainting procedure for smoothing the skin regions. So, from the visual results it is observed that the proposed method perfectly removes the hair region.

3.3 | Objective evaluation

The visual or subjective evaluation is not enough to estimate the performance of the system. Thus, the objective evaluation is useful to estimate the performance of various algorithms individually. So, it is possible to compare the performance of proposed system with the conventional approaches easily.

3.3.1 | Filtering and hair removal

This article considers the nine-objective parameters for evaluating the performance of Hair removal approach. The parameters are categorized into three various groups. The first group contains structural similarity (SSIM) index, peak signal-to-noise ratio (PSNR), mean squared error (MSE), and root mean squared error (RMSE) metrics, these are pixel-wise analysis metrics. The second group contains the universal quality image index (UQI) and multi-scale SSIM (MS-SSIM) metrics, these are local statistical features. Finally, the third group contains PSNR- human visual system (HVS), PSNR-HVS-M and visual information fidelity (VIF) metrics, these are metrics are used to compare the output of simulation with HVS. The RMSE and MSE values should be low and remaining all metrics should be high, this scenario indicates hair removed reconstructed image quality increased, so system archives the best performance.

Table 5 compares the performance of proposed method with various conventional approaches with respect to the nine-parameters. Here, the MSE and RMSE of proposed method is low, it means the reconstructed output image contains less errors. SSIM and MSSSIM of proposed method is high, it indicates the hair removed reconstructed output image is like the input image. Finally, PSNR, VIF, UQI, and PSNR-HVS-M

| Cancer type | MEL | NV | BCC | AKIES |
|-----------------------|-----|----|------|-------|
| Test images | | | | |
| Hair removed outcomes | | | | |
| Segmented outcomes | | | | |
| Cancer type | BKL | DF | VASC | SCC |
| Test images | | | | |
| Hair removed outcomes | | | | |
| Segmented outcomes | | | | |

FIGURE 11 Artefact removal image with segmented outcome

parameters are high, it means the proposed system gives the better-quality hair removed reconstructed image. It is proved that “the proposed HGF-CCL method gives the optimal performance of all parameters compared to the CTI (Gessert et al., 2018), CUOD (Guisous et al., 2019), HI (Gutman et al., 2016), FGF-CEF (Khan et al., 2020), BHF (Hardie et al., 2018), ADF (Hawas et al., 2020), and DLCNN (Hekler et al., 2019)”.

3.3.2 | Segmentation analysis

This article considers the six objective parameters for calculating the FrCN segmentation efficiency. They are segmentation accuracy (S-ACC), sensitivity (SEN), specificity (SPE), Jaccard index (JAC), Matthew correlation coefficient (MCC), and dice coefficient (DIC). The Jaccard index, also

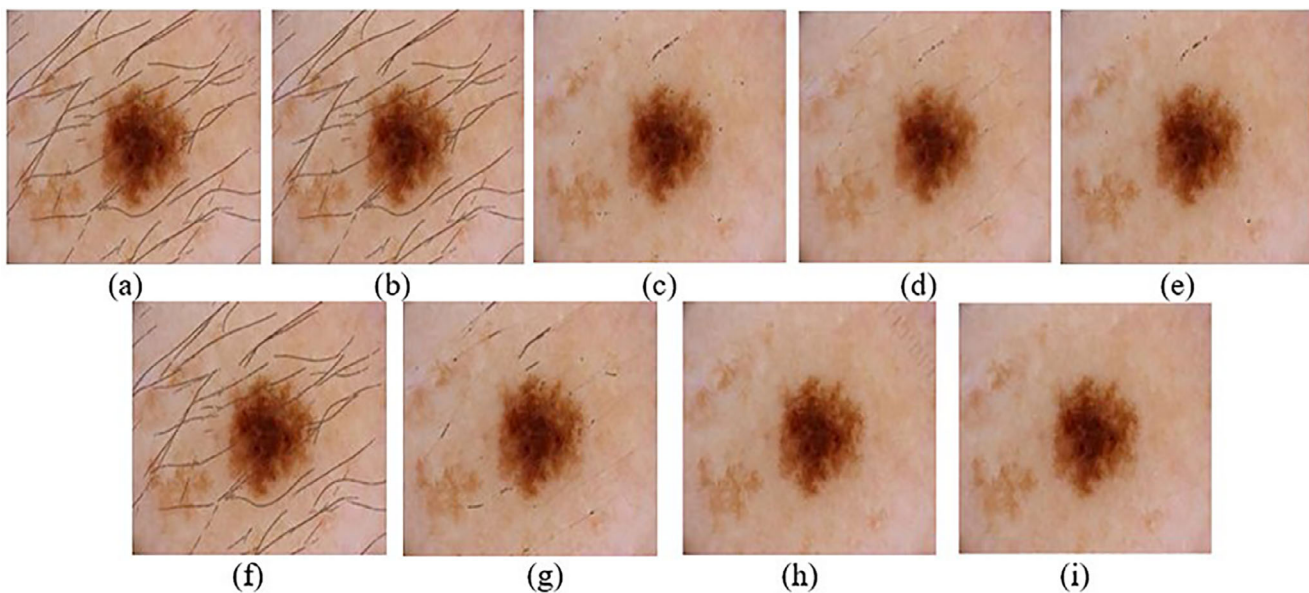


FIGURE 12 Obtained results using hair artefact removal methods. (a) Test input image. (b) CTI (Goyal et al., 2020). (c) CUOD (Guisous et al., 2019). (d) HI (Gutman et al., 2016). (e) FGF-CEF (Khan et al., 2020). (f) BHF (Hardie et al., 2018). (g) ADF (Hawas et al., 2020). (h) DLCNN (Hekler et al., 2019). (i) HGF-CCL

TABLE 5 Performance comparison of various hair removal methods

| Metric | CTI (Goyal et al., 2020) | CUOD (Guisous et al., 2019) | HI (Gutman et al., 2016) | DLCNN (Hekler et al., 2019) | FGF CEF (Khan et al., 2020) | BHF (Hardie et al., 2018) | ADF (Hawas et al., 2020) | HGF-CCL |
|------------|--------------------------|-----------------------------|--------------------------|-----------------------------|-----------------------------|---------------------------|--------------------------|---------|
| MSE | 55.311 | 221.346 | 175.303 | 27.47 | 404.366 | 103.903 | 258.347 | 21.43 |
| SSIM | 0.921 | 0.864 | 0.890 | 0.926 | 0.851 | 0.885 | 0.867 | 0.953 |
| PSNR | 33.096 | 26.570 | 29.158 | 35.17 | 27.001 | 29.87 | 26.080 | 41.28 |
| RMSE | 6.318 | 13.287 | 11.032 | 4.790 | 15.485 | 9.207 | 14.226 | 2.102 |
| VIF | 0.592 | 0.509 | 0.531 | 0.525 | 0.402 | 0.499 | 0.526 | 0.637 |
| UQI | 0.997 | 0.992 | 0.995 | 0.997 | 0.990 | 0.996 | 0.991 | 0.999 |
| MSSSIM | 0.955 | 0.875 | 0.945 | 0.998 | 0.917 | 0.934 | 0.870 | 0.999 |
| PSNR-HVS-M | 33.005 | 25.519 | 28.445 | 36.802 | 26.248 | 29.404 | 25.078 | 42.945 |
| PSNR-HVS | 32.186 | 25.065 | 27.826 | 35.168 | 25.738 | 28.681 | 24.628 | 43.248 |

recognized as the Jaccard similarity correlation, is a data point which is used to calculate the similarity and diversification of tested samples. The Matthews correlation coefficient is a more accurate statistical rate which generates a high score unless the prediction conducted in all four confusion matrix classifications. The Dice similarity coefficient, also recognized as the Sorenson-Dice index or plainly the Dice coefficient, is a numerical technique for evaluating the similarity of two data sets. Highest values of these metrics indicate the system segments the skin lesion perfectly and achieves the optimal performance.

From Table 6, it is observed that the proposed method gives the best segmentation performance compared to various conventional approaches such as CDNN (Maiorino et al., 2016), ResNet (Murphree & Ngufor, 2017) and U-Net (Nida et al., 2019). These works are participated in task-1 of ISIC-2017 challenges, the drawbacks of these approaches are presented in the literature. The proposed method also compared with the non-participated and published work of skin cancer segmentation methods such as PSPNet (Pacheco et al., 2019), DTL (Rahmat et al., 2016) and U-Net (Sau et al., 2018). Compared to all these works, the proposed FrCN segmentation obtained the best segmentation results because initially hair and noise is removed from the skin lesions. Here, The SEN parameter indicates the percentage of pixels that are perfectly segmented. The proposed FrCN segmentation achieves the highest segmentation sensitivity, thus it is accurately segmented the skin lesion pixels. The FrCN method achieves the highest specificity, thus it is accurately classified the non-skin lesion pixels and those pixels are not segmented. The FrCN method gives the highest segmentation accuracy, thus it accurately segments the skin lesion. The FrCN method gives the highest DIC, thus it

TABLE 6 Performance comparison of various segmentation approaches for ISIC challenges

| Dataset | Rank | Method | SEN (%) | SPE (%) | DIC | JAC | S-ACC (%) | MCC |
|-----------|-----------------|-------------------------------|---------|---------|-------|-------|-----------|-------|
| ISIC-2017 | 1 | CDNN (Maiorino et al., 2016) | 82.50 | 97.50 | 84.90 | 76.50 | 93.40 | 95.39 |
| | 2 | FCRN (Li & Shen, 2018) | 82.00 | 97.80 | 84.70 | 76.20 | 93.20 | 95.20 |
| | 3 | ResNet (Nida et al., 2019) | 80.20 | 98.50 | 84.40 | 76.00 | 93.40 | 96.93 |
| ISIC-2017 | Not participate | PSPNet (Pacheco et al., 2019) | 85.34 | 98.88 | 86.73 | 78.83 | 95.23 | 96.29 |
| | | DTL (Rahmat et al., 2016) | 90.38 | 99.23 | 90.46 | 82.48 | 96.37 | 97.38 |
| | | U-Net (Sau et al., 2018) | 93.86 | 99.40 | 93.23 | 86.35 | 96.45 | 97.45 |
| ISIC-2019 | | FrCN | 98.95 | 99.44 | 95.62 | 95.68 | 97.28 | 97.90 |

TABLE 7 Feature extraction performance comparison with conventional approaches

| Method | ACC (%) | SEN (%) | SPEC (%) | Precision (%) | AUC |
|-----------------------|---------|---------|----------|---------------|-------|
| Jeremy Kawahara | 98 | 54.2 | 98.1 | 24.1 | 0.895 |
| LFN (Li & Shen, 2018) | 91.4 | 66.56 | 91.5 | 40.9 | 0.833 |
| Proposed-DRB | 99.23 | 89.49 | 99.37 | 84.89 | 0.91 |

TABLE 8 Classification performance comparison with conventional approaches

| Method | C-ACC (%) | SEN (%) | SPEC (%) | Precision (%) | AUC |
|-------------------------------------|-----------|---------|----------|---------------|--------|
| DLCNN (Zhang, 2017) | 81 | 74 | 84 | 77 | 0.834 |
| DenseNet 201 (Samuel & Kanna, 2018) | 85.8 | 82.4 | 89.35 | 84.67 | 0.893 |
| CNN-DG (Xie et al., 2019) | 66.2 | 66.2 | 95.2 | 78 | 0.915 |
| MCM-CNN (Zortea et al., 2017) | 95.39 | 93.24 | 94.58 | 92.28 | 0.902 |
| Proposed Transfer learning | 98.92 | 98.8 | 97.56 | 98.36 | 0.9636 |

accurately segments the skin lesions, and they were matched with the ground-truth images. The FrCN method gives the highest JAC, thus FrCN achieved the optimal pixel-wise segmentation performance and perfectly intersected with the ground truth masks. The FrCN method gives the highest MCC, thus FrCN achieved the maximum correlation between segmented skin lesion pixels and annotated images. From the Table 4, it is proved that the proposed method gives the optimal performance for individual benign, melanoma and overall-eight diseases. The FrCN method directly extracts the detailed features for each pixel and segments the region accurately through the convolutional layers and the performance of the proposed method increased by optimizing the training loss.

3.3.3 | Feature extraction analysis

Table 7 compares the feature extraction performance proposed method conventional FCRN (Li & Shen, 2018) and unpublished work “Jeremy Kawahara” on ISIC-2017 challenge dataset. Here, “Jeremy Kawahara” team gained the first position and FCRN (Li & Shen, 2018) achieved the second position in task 2 of ISIC-2017 challenge. Here, the FCRN (Li & Shen, 2018) method utilizes the lesion feature network (LFN) based CNN for solving the solution to ISIC challenge. But the major drawbacks of these two methods was, they are extracted the only ABCDE based features. They were not extracted the disease dependent and disease specific features. Thus, to overcome these problems the proposed DRB feature extraction utilizes the Intra-DDM based DRB, Inter-DDM based DRB, and DSM based DRB modules and achieved the optimal performance.

3.3.4 | Classification analysis

This work considered classification accuracy (C-ACC), SPEC, SEN, precision, and AUC parameters for analysing the classification performance of eight diseases. The conventional approaches utilized both machine learning and DL approaches for classifying the skin cancers.

Table 8 compares the classification performance of proposed transfer learning method with conventional basic DL approaches. The conventional DLCNN (Xie et al., 2019), CNN-DG (Zhang, 2017), DenseNet 201 (Samuel & Kanna, 2018) and MCM-CNN (Zortea et al., 2017) based

approaches utilized the basic regularizers such as lasso regression and ridge regression. All the experiments are carried out on ISIC-2019 dataset. If the input image resolution increases, then the number of instances were reduced, and these optimizations were not performed accurate optimization. In these methods, authors used CNN with novel regularizer. These methods suffer with multiple drawbacks, they are it cannot be utilized for neither feature reduction nor feature selection and the computation complexity of these methods also high with more time consumption. Thus, to overcome these drawbacks, the proposed method developed with the HGG-CCL based hair removal, FrCN segmentation, Disease dependent and disease specific feature extraction using DRB and finally transfer learning-based classification. All the DL methods are optimized by analysing the total loss function and the performance of the proposed method is improved compared to all conventional approaches.

3.4 | Comparison with ISIC-2019 challenge

Table 9 compares the performance of the proposed method with ECNN (Sekaran, 2019) and RSD (Zou et al., 2018) methods on ISIC-2018 challenge dataset. And the performance of proposed method also compared with the RSD (Zou et al., 2018) and unpublished works of leaderboard such as “Cancerless and ForCure” methods. These methods are suffering with the loss balancing problems. By comparing with leaderboard participants, it was proved that the proposed method has potentially dominant mechanism than other state of art approaches and can achieve the highest position in leaderboard. Thus, the proposed method achieves the better performance as compared to the conventional approaches because the proposed method utilizes the transfer learning models and advanced loss optimization methods.

3.5 | Ablation study

The ablation study deals with the removing of removing of some layers in the DL mechanism and checks the performance of the system with respect to various objective evaluation. Table 10 illustrates detailed analysis of Ablation Study with respect to the various scenarios by the elimination of multiple convolutional layers. The skin lesions are not perfectly segmented by reducing the Number of layers in FrCN segmentation process. Hence, in this scenario the classification of eight disease performance is reduced and segmentation performance also reduced as follows: SEN is 88.24, SPE is 86.95, ACC is 84.45, DIC is 86.77, JAC is 85.63 and MCC is 83.28. if the any one of the modules such as Intra based DRB, inter based DRB and DSM based DRB is eliminated from feature extraction procedure also reduced the classification performance. Because the accurate features of eight diseases were not perfectly extracted and the dependency, similarity between diseases also not extracted effectively. Finally, the classification performance of the system also reduced by eliminating the GoogLeNet or VGGNet or ResNet modules from the transfer

TABLE 9 Performance comparison of various classification approaches for ISIC challenges

| Dataset | Method | Rank | C-ACC (%) | SEN (%) | SPEC (%) | AUC |
|-----------|------------------------|------|-----------|---------|----------|--------|
| ISIC-2018 | ECNN (Sekaran, 2019) | 1 | 88.5 | 83.3 | 98.6 | 0.983 |
| | RSD (Zou et al., 2018) | 2 | 85.6 | 80.9 | 98.4 | 0.987 |
| ISIC-2019 | RSD (Zou et al., 2018) | 1 | 63.6 | 50.7 | 97.7 | 0.923 |
| | Cancerless | 2 | 63.8 | 53.1 | 97.4 | 0.913 |
| | ForCure | 3 | 64.8 | 53.4 | 97.4 | 0.914 |
| | Proposed | — | 98.92 | 98.8 | 97.56 | 0.9636 |

TABLE 10 Obtained performance metrics with ablation study

| Scenario | ACC (%) | SEN (%) | SPEC (%) | Precision (%) |
|------------------------------------|---------|---------|----------|---------------|
| By reducing the few layers in FrCN | 93.31 | 73.13 | 95.37 | 62.5 |
| By eliminating Inter-DDM based DRB | 94.52 | 74.55 | 96.55 | 73.62 |
| By eliminating Intra-DDM based DRB | 95.32 | 79.88 | 97.56 | 80.36 |
| By eliminating DSM based DRB | 92.99 | 70.44 | 96.34 | 82.47 |
| By eliminating GoogLeNet | 94.41 | 89.93 | 96.12 | 83.48 |
| By eliminating VGGNet | 95.35 | 74.39 | 95.93 | 85.69 |
| By eliminating ResNet | 95.73 | 95.23 | 96.82 | 89.73 |

learning process. Because the reduction of these transfer learning models resulted in the reduction of the individual type of diseases classification capability.

4 | CONCLUSION

In this article, SLDC using FrCN-based DL with transfer learning is developed to classify eight types of skin cancers from the ISIC-2019 challenge dataset with the advantage of hair and noise removal and appropriate lesion segmentation. Initially, HGF is used to remove the noises from test images, followed by CCL based fast march inpainting procedure to remove the unwanted hair from skin lesions. Then, FrCN based segmentation method is applied to localize the area of effected skin lesion with improved accuracy. Next, inter-DDM based DRB, intra-DDM based DRB, and DSM-based DRB models are used to extract the disease dependent and disease specific hierarchical features. Finally, the transfer learning models are trained with these features individually. Here, GoogLeNet, VGGNet and ResNet based transfer learning models are used for the classification of skin lesions. In addition, the transfer learning model performance has been optimized using the Gamma regularizer. Further, the computation complexity of all the proposed models also optimized by the total loss analysis and resulted in less time for training of individual diseases. The performance of the proposed method is computed w.r.t. nine-parameters for hair removal process, six-parameters for segmentation process and five-parameters for classification operation. Form the obtained results, it is proven that proposed hybrid model produced the enhanced performance as compared to many existing approaches for all parameters. Finally, the performance of proposed hybrid mode also compared with leadership leaderboard of ISIC-2019 challenge and resulted in optimal performance. This work can be further extended to implement the optimal feature selection algorithms using natural bio-inspired optimization algorithms for further improvement in S-ACC and C-ACC.

CONFLICT OF INTEREST

The authors declare no conflicts of interest.

DATA AVAILABILITY STATEMENT

Not applicable.

ORCID

P. Bharat Siva Varma  <https://orcid.org/0000-0003-1708-045X>

Pala Mahesh Kumar  <https://orcid.org/0000-0002-8591-5781>

REFERENCES

- Abbas, A. A., & Abu-Almash, F. S. (2020). Skin lesion border detection based on optimal statistical model using optimized colour channel. *Journal of Autonomous Intelligence*, 3(1), 18–26.
- Abraham, N., & Khan, N. M. (2019). A novel focal tversky loss function with improved attention u-net for lesion segmentation. In *2019 IEEE 16th international symposium on biomedical imaging (ISBI 2019)* (pp. 683–687). IEEE.
- Alfed, N., & Khelifi, F. (2017). Bagged textural and color features for melanoma skin cancer detection in dermoscopic and standard images. *Expert Systems with Applications*, 90, 101–110.
- Amin, J., Sharif, A., Gul, N., Anjum, M. A., Nisar, M. W., Azam, F., & Bukhari, S. A. C. (2020). Integrated design of deep features fusion for localization and classification of skin cancer. *Pattern Recognition Letters*, 131, 63–70.
- Bakay, M. S., & Ağbulut, Ü. (2021). Electricity production based forecasting of greenhouse gas emissions in Turkey with deep learning, support vector machine and artificial neural network algorithms. *Journal of Cleaner Production*, 285, 125324.
- Balaji, V. R., Suganthi, S. T., Rajadevi, R., Kumar, V. K., Balaji, B. S., & Pandiyan, S. (2020). Skin disease detection and segmentation using dynamic graph cut algorithm and classification through naive Bayes classifier. *Measurement*, 163, 107922.
- Bi, L., Kim, J., Ahn, E., & Feng, D. (2017). Automatic skin lesion analysis using large-scale dermoscopy images and deep residual networks. *arXiv*, 1703, 04197.
- Bibiloni, P., González-Hidalgo, M., & Massanet, S. (2017). Skin hair removal in dermoscopic images using soft color morphology. In *Conference on artificial intelligence in medicine in Europe* (pp. 322–326). Springer.
- Bissoto, A., Perez, F., Ribeiro, V., Fornaciali, M., Avila, S., & Valle, E. (2018). Deep-learning ensembles for skin-lesion segmentation, analysis, classification: RECOD titans at ISIC challenge 2018. *arXiv*, 1808, 08480.
- Chatterjee, S., Dey, D., & Munshi, S. (2019). Integration of morphological preprocessing and fractal based feature extraction with recursive feature elimination for skin lesion types classification. *Computer Methods and Programs in Biomedicine*, 178, 201–218.
- Chatterjee, S., Dey, D., Munshi, S., & Gorai, S. (2019). Extraction of features from cross correlation in space and frequency domains for classification of skin lesions. *Biomedical Signal Processing and Control*, 53, 101581.
- Codella, N., Rotemberg, V., Tschandl, P., Celebi, M. E., Dusza, S., Gutman, D., & Halpern, A. (2019). Skin lesion analysis toward melanoma detection 2018: A challenge hosted by the international skin imaging collaboration (isic). *arXiv*, 1902, 03368.
- Gessert, N., Sentker, T., Madesta, F., Schmitz, R., Kniep, H., Baltruschat, I., & Schlaefer, A. (2018). Skin lesion diagnosis using ensembles, unscaled multi-crop evaluation and loss weighting. *arXiv*, 1808, 01694.
- Goyal, M., Knackstedt, T., Yan, S., & Hassanpour, S. (2020). Artificial intelligence-based image classification for diagnosis of skin cancer: Challenges and opportunities. *Computers in Biology and Medicine*, 127, 104065.

- Guisous, A. E. (2019). Skin lesion classification using deep neural network. *arXiv*, 1911, 07817.
- Gutman, D., Codella, N. C., Celebi, E., Helba, B., Marchetti, M., Mishra, N., & Halpern, A. (2016). Skin lesion analysis toward melanoma detection: A challenge at the international symposium on biomedical imaging (ISBI) 2016, hosted by the international skin imaging collaboration (ISIC). *arXiv*, 1605, 01397.
- Hardie, R. C., Ali, R., De Silva, M. S., & Kebede, T. M. (2018). Skin lesion segmentation and classification for ISIC 2018 using traditional classifiers with hand-crafted features. *arXiv*, 1807, 07001.
- Hawas, A. R., Guo, Y., Du, C., Polat, K., & Ashour, A. S. (2020). OCE-NGC: A neutrosophic graph cut algorithm using optimized clustering estimation algorithm for dermoscopic skin lesion segmentation. *Applied Soft Computing*, 86, 105931.
- Hekler, A., Utikal, J. S., Enk, A. H., Hauschild, A., Weichenthal, M., Maron, R. C., Berking, C., Haferkamp, S., Klode, J., Schadendorf, D., Schilling, B., Holland-Letz, T., Izar, B., von Kalle, C., Fröhling, S., Brinker, T. J., Schmitt, L., Peitsch, W. K., Hoffmann, F., ... Thiem, A. (2019). Superior skin cancer classification by the combination of human and artificial intelligence. *European Journal of Cancer*, 120, 114–121.
- Hemalatha, R. J., Babu, B., Dhivya, A. J. A., Thamizhvani, T. R., Joseph, J. E., & Chandrasekaran, R. (2017). A comparison of filtering and enhancement methods in malignant melanoma images. In *2017 IEEE international conference on power, control, signals and instrumentation engineering (ICPCSI)* (pp. 2704–2710). IEEE.
- Jagadesh, B. N., Rao, K. S., & Satyanarayana, C. (2020). A unified approach for skin colour segmentation using generic bivariate Pearson mixture model. *International Journal of Advanced Intelligence Paradigms*, 15(1), 17–31.
- Kang, D., Kim, S., & Park, S. (2018). Flow-guided hair removal for automated skin lesion identification. *Multimedia Tools and Applications*, 77(8), 9897–9908.
- Khan, A. H., Iskandar, D. N. F. A., Al-Asad, J. F., & El-Nakla, S. (2021). Classification of Skin Lesion with Hair and Artifacts Removal using Black-hat Morphology and Total Variation. *International Journal of Computing and Digital Systems*, 10(1), 597–604. <http://dx.doi.org/10.12785/ijcds/100157>
- Li, X., Yang, S., Fan, R., Yu, X., & Chen, D. (2018). Discrimination of soft tissues using laser-induced breakdown spectroscopy in combination with k nearest neighbors (kNN) and support vector machine (SVM) classifiers. *Optics & Laser Technology*, 102, 233–239.
- Li, Y., & Shen, L. (2018). Skin lesion analysis towards melanoma detection using deep learning network. *Sensors*, 18(2), 556.
- Mahbod, A., Schaefer, G., Wang, C., Dorffner, G., Ecker, R., & Ellinger, I. (2020). Transfer learning using a multi-scale and multi-network ensemble for skin lesion classification. *Computer Methods and Programs in Biomedicine*, 193, 105475.
- Maiorino, A., De Simone, C., Perino, F., Calderola, G., & Peris, K. (2016). Melanoma and non-melanoma skin cancer in psoriatic patients treated with high-dose phototherapy. *Journal of Dermatological Treatment*, 27(5), 443–447.
- Mohamed, E. H., & El-Behaidy, W. H. (2019). Enhanced skin lesions classification using deep convolutional networks. In *2019 ninth international conference on intelligent computing and information systems (ICICIS)* (pp. 180–188). IEEE.
- Murphree, D. H., & Ngufor, C. (2017). Transfer learning for melanoma detection: Participation in ISIC 2017 skin lesion classification challenge. *arXiv*, 1703, 05235.
- Nida, N., Irtaza, A., Javed, A., Yousaf, M. H., & Mahmood, M. T. (2019). Melanoma lesion detection and segmentation using deep region based convolutional neural network and fuzzy C-means clustering. *International Journal of Medical Informatics*, 124, 37–48.
- Nozdrym-Plotnicki, A., Yap, J., & Yolland, W. (2018). Ensembling convolutional neural networks for skin cancer classification. International Skin Imaging Collaboration (ISIC) Challenge on Skin Image Analysis for Melanoma Detection. MICCAI.
- Pacheco, A. G., Ali, A. R., & Trappenberg, T. (2019). Skin cancer detection based on deep learning and entropy to detect outlier samples. *arXiv*, 1909, 04525.
- Rahmat, R. F., Chairunnisa, T., Gunawan, D., & Sitompul, O. S. (2016). Skin color segmentation using multi-color space threshold. In *2016 3rd international conference on computer and information sciences (ICCOINS)* (pp. 391–396). IEEE.
- Salido, J. A. A., & Ruiz, C., Jr. (2017). Using morphological operators and inpainting for hair removal in dermoscopic images. In *Proceedings of the computer graphics international conference* (pp. 1–6). ACM digital library. <https://dl.acm.org/doi/10.1145/3095140.3095142>
- Samuel, R. D., & Kanna, B. R. (2018). Tuberculosis (TB) detection system using deep neural networks. *Neural Computing and Applications*, 31(5), 1533–1545.
- Sau, K., Maiti, A., & Ghosh, A. (2018). Preprocessing of skin cancer using anisotropic diffusion and sigmoid function. In *Advanced computational and communication paradigms* (pp. 51–61). Springer.
- Sekaran, K. (2019). Deep learning convolutional neural network (CNN) with Gaussian mixture model for predicting pancreatic cancer. *Multimedia Tools and Applications*, 79(15), 233–247.
- Sengupta, S., Mittal, N., & Modi, M. (2020). Improved skin lesions detection using color space and artificial intelligence techniques. *Journal of Dermatological Treatment*, 31(5), 511–518.
- Sharma, V., Garg, A., & Thenmalar, S. (2020). A survey on classification of malignant melanoma and benign skin lesion by using machine learning techniques. *Easy Chair Preprint*, 2611.
- Soomro, S., Munir, A., & Choi, K. N. (2019). Fuzzy c-means clustering based active contour model driven by edge scaled region information. *Expert Systems with Applications*, 120, 387–396.
- Sun, Q., Huang, C., Chen, M., Xu, H., & Yang, Y. (2021). Skin lesion classification using additional patient information. *BioMed Research International*, 2021(2021), 1–6.
- Talavera-Martinez, L., Bibiloni, P., & González-Hidalgo, M. (2019). Comparative study of dermoscopic hair removal methods. In *ECCOMAS thematic conference on computational vision and medical image processing* (pp. 12–21). Springer.
- Talavera-Martinez, L., Bibiloni, P., & Gonzalez-Hidalgo, M. (2020). Hair segmentation and removal in dermoscopic images using deep learning. *IEEE Access*, 9, 2694–2704.
- Tan, T. Y., Zhang, L., Neoh, S. C., & Lim, C. P. (2018). Intelligent skin cancer detection using enhanced particle swarm optimization. *Knowledge-Based Systems*, 158, 118–135.
- Thomsen, K., Iversen, L., Titlestad, T. L., & Winther, O. (2020). Systematic review of machine learning for diagnosis and prognosis in dermatology. *Journal of Dermatological Treatment*, 31(5), 496–510.
- Toossi, M. T. B., Pourreza, H. R., Zare, H., Sigari, M. H., Layegh, P., & Azimi, A. (2013). An effective hair removal algorithm for dermoscopy images. *Skin Research and Technology*, 19(3), 230–235.
- Xie, H., Zhang, L., Lim, C. P., Yu, Y., Liu, C., Liu, H., & Walters, J. (2019). Improving K-means clustering with enhanced firefly algorithms. *Applied Soft Computing*, 84, 105763.
- Zhang, G. (2017). Deep learning based feature representation for automated skin Histopathological image annotation. *Multimedia Tools and Applications*, 77(8), 9849–9869.

- Zorteia, M., Flores, E., & Scharcanski, J. (2017). A simple weighted thresholding method for the segmentation of pigmented skin lesions in macroscopic images. *Pattern Recognition*, 64, 92–104.
- Zou, J., Ma, X., Zhong, C., & Zhang, Y. (2018). Dermoscopic image analysis for ISIC challenge 2018. *arXiv*, 1807, 08948.

AUTHOR BIOGRAPHIES



P. Bharath Siva Varma is currently working in the Department of Computer Science and Engineering at the Sagi Rama Krishnam Raju Engineering College, Bhimavaram, Andhra Pradesh, India. He has completed B.Tech in Information Technology from the Andhra University in the year of 2009 and M.Tech graduated from the Jawaharlal Nehru Technological University, Kakinada, Andhra Pradesh in 2011. He obtained Ph.D. from the Koneru Lakshmaiah Education Foundation, Vaddeswaram, Andhra Pradesh, India in the year of 2021. He had more than 10 years of teaching experience. He has published more than 10 journals and 7 conference publications at national and international level. He has guided 40+ undergraduate projects and 25+ postgraduate projects during his academic career. His research interested areas are machine learning and artificial intelligence in medical imaging and cloud security.



Siddartha Patru is currently working as a Data Scientist in World Bank Group, Washington D.C. He has completed a master's in Business Analytics from the Drexel University, Philadelphia, PA, and B.E. Mechanical Engineer from the Sagi Rama Krishnam Raju Engineering College, Bhimavaram, Andhra Pradesh. He has 10+ years of experience in data science-related projects. His research interests are data science, machine learning, artificial intelligence, and blockchain for social good.



Suman Mishra is currently working as Professor and Head of the Department of Electronics and Communication Engineering in CMR Engineering College, Hyderabad. He has obtained his under-graduate degree in Electronics and Communication Engineering from The Institution of Engineers (India), master's degree M.E. in Applied Electronics from University of Madras and Ph.D. from the Sathyabama University, Chennai. He has over 20 years of teaching and research experience, and 4 years of industrial experience. He is currently guiding one Ph.D. research scholar, 10 M.Tech dissertations and 45 B.Tech projects. He has published his research findings in 20 journals and 6 conferences both in national and international level. He has authored two textbooks Electronic Devices and Wireless Sensor Networks. He is the lifetime member of IE (India), ISTE and IAENG. He is the reviewer for two International Journals and has been a member of technical committees of two International Conferences. He has also acted as examiner for Ph.D. theses. His research interest includes medical image processing, sensor networks soft computing.



B. Srinivasa Rao currently working as Professor at the Koneru Lakshmaiah Education Foundation, Vaddeswaram, Andhra Pradesh, India. He has completed Ph.D. from Acharya Nagarjuna University, Guntur, Andhra Pradesh, India. He obtained M.Tech from the Jawaharlal Nehru Technological University, Anantapur, Andhra Pradesh, India. He has done B.Tech from the Acharya Nagarjuna University, Guntur, Andhra Pradesh, India. He has 25+ years of teaching and research experience. He has published 20 journals, and 10 conferences at national and international level. He has also guided several Ph.D. scholars under his supervision. His research interested areas are medical imaging, computer networks, and internet of things.



Pala Mahesh Kumar received B.Tech in ECE from the Jawaharlal Nehru Technological University, Hyderabad. He has done M.Tech (embedded systems) from the Jawaharlal Nehru Technological University, Hyderabad, Telangana, India. Currently, he is in association with SAK Informatics, Hyderabad. He had 10+ years of experience in R&D and technical content writing. He acted as a mentor for more than 200 undergraduate projects and 70 postgraduate projects. His research interested areas are machine learning, and deep learning with the applications in image, video, and speech processing. He is a member of IEEE.



Namani Vamshi Krishna currently pursing Ph.D. in Electronics and Communication Engineering from the Nirwan University, Jaipur, Rajasthan, India. He has received the master's degree in Communication Systems from the Jawaharlal Nehru Technological University, Hyderabad. He has completed bachelor's degree from the Vardaman College Of Engineering, Hyderabad. He is currently working as AI Engineer at SAK Informatics, Hyderabad. He has published 10 international research articles in the field of image processing, VLSI, and communication. His research interested areas are artificial intelligence, and deep learning in image processing, and communication applications.

How to cite this article: Varma, P. B. S., Paturu, S., Mishra, S., Rao, B. S., Kumar, P. M., & Krishna, N. V. (2022). SLDCNet: Skin lesion detection and classification using full resolution convolutional network-based deep learning CNN with transfer learning. *Expert Systems*, 39(9), e12944. <https://doi.org/10.1111/exsy.12944>

Copyright of Expert Systems is the property of Wiley-Blackwell and its content may not be copied or emailed to multiple sites or posted to a listserv without the copyright holder's express written permission. However, users may print, download, or email articles for individual use.